OH* Chemiluminescence Images of Detonations Propagating through the Annular Channel of a Nonpremixed Rotating Detonation Engine

Brent A. Rankin[1], Daniel R. Richardson[2], Andrew W. Caswell[3], Andrew G. Naples[4],
John L. Hoke[4], and Frederick R. Schauer[3]
[1]National Research Council, Air Force Research Laboratory
[2]Spectral Energies
[3]Air Force Research Laboratory
[4]Innovative Scientific Solutions Inc.
Dayton, OH, USA

1 Introduction

Rotating detonation engines (RDEs) have received increased attention over the past few years because of the potential for higher thermodynamics efficiencies associated with pressure gain combustion, continuous presence of a detonation after ignition, and compact design. Investigations of RDEs are relevant to a range of aerospace applications. Rotating detonation engines provide a possible alternative to existing rocket engines for propulsion. Turbines driven by RDEs offer the potential for increasing pressure ratios, increasing thermodynamics efficiencies, and reducing fuel consumption. Significant progress has been made in the research and development of RDEs over the past few years[1-5]. Several significant challenges need to be addressed regarding RDE operation and performance. One of the most important opportunities involves identifying a fuel and air injection scheme that optimizes mixing and reduces pressure losses across the inlet of RDEs so that the pressure gain associated with detonations can be realized. Reducing these pressure losses typically results in large oscillations in the air and fuel plenums upstream of the detonation channel[2].

Investigations of the flow[3] within the detonation channel are useful for understanding the fuel and air mixing, unsteady reacting flow processes, and detonation structure affecting the overall RDE performance. Comparison of existing and emerging RDE simulation results[4,5] with non-intrusive two-dimensional imaging measurements (e.g. OH* chemiluminescence) can lead to new fundamental insights into continuously propagating detonations and advanced RDE designs. The improved understanding provides a foundation for optimizing the design of RDEs to minimize pressure loss across the inlet and maximize pressure gain, combustion efficiency, and thrust.

The detonation propagating through the annular channel of an optically accessible nonpremixed rotating detonation engine is visualized using OH* chemiluminescence imaging in this work. The fuel and air are injected from separate streams and partially premix in the channel in front of the detonation wave. The OH* chemiluminescence images allow observation of the size and shape of the detonation structure, trailing edge oblique shock wave, and possible presence of deflagration between the fuel fill region and expansion region containing detonated products. The OH* chemiluminescence images are useful for evaluating the effects of the air mass flow rate, equivalence ratio, air injection area, and fuel injection scheme on the detonation structure and its corresponding impact on RDE operation and performance. Measurements of the time-dependent and time-averaged static pressure along the length of the annular detonation channel are acquired with sufficient spatial resolution to understand the effects of the pressure gradient on the detonation structure and RDE performance. The OH*

Correspondence to: brent.a.rankin@gmail.com

chemiluminescence images are useful for evaluating RDE models and simulations, improving fundamental understanding of the detonation structure in nonpremixed RDEs, and identifying critical design parameters that influence RDE operation and performance.

2 Experimental Methods

A schematic and photograph of the optically accessible RDE are shown in Fig. 1. Air is injected from a plenum through a circumferential slot (123 mm diameter) into an annular detonation channel. The height of the air slot (0.89, 1.78, or 3.56 mm) is varied to change the air injection area (3.46, 6.92, or 13.83 cm^2). Fuel is injected from a separate plenum through holes evenly spaced on a circle with a circumference (134 mm) located near the inner edge of the annular detonation channel. The diameter (0.71 or 0.89 mm) and number (80 or 120) of the fuel injection holes is varied to change the fuel injection area (0.48 or 0.74 cm2). The inner and outer diameters of the annular detonation channel are 138.7 mm (5.46 in) and 153.9 mm (6.06 in.), respectively, resulting in a channel width of 7.6 mm (0.30 in.). The height of the annular detonation channel is 101.6 mm (4.0 in.). A quartz (GE124) tube (2.54 cm thick) is used as the outerbody to allow for optical accessibility of the annular detonation channel. The rotating detonation engine is operated by injecting hydrogen and air from separate plenums. The fuel and air mass flow rates were metered upstream of the respective plenums by using two sonic nozzles. The air mass flow rate is varied from 0.15 – 0.86 kg/s (20 – 110 lbm/min). The hydrogen and air mass flow rates would result in an equivalence ratio ranging from 0.70 – 1.30 if the hydrogen and air were premixed prior to injection.

The RDE is operated using a sequence that involves establishing the air and fuel flow followed by initiating the detonation. The detonation in the annular channel is initiated using a small detonation tube. Hydrogen and oxygen flow into the small detonation tube (6.35 mm diameter, 63.5 mm long), and the mixture is spark ignited. The deflagration-to-detonation transition occurs in the small tube, and three consecutive pulsed detonations exit into the annular detonation channel of the RDE to initiate the detonation in the channel. The pressure in the fuel and air plenums initially increases due to the backpressure effects associated with the detonation in the channel. Data are reported after steady state conditions have been achieved in the plenums.
Images of OH* chemiluminescence are acquired using a high speed camera (Photron SA-5 CMOS) and UV intensifier (LaVision IRO). The images are acquired using a 45 mm lens (f/1.8) and band-pass filter (320 +/- 20 nm). The spatial resolution of the images is approximately 0.31 mm/pixel. The images are collected with an exposure time of 300 ns at a sample frequency of 20 kHz. Images are recorded for 0.5 s resulting in 10,000 images for each operating condition. The spatial and temporal resolutions are sufficient to minimize blurring effects (to less than 3 pixels) associated with imaging the high speed detonation wave. A gain of 73 and 64 on the intensifier are used for the low (0.15 and

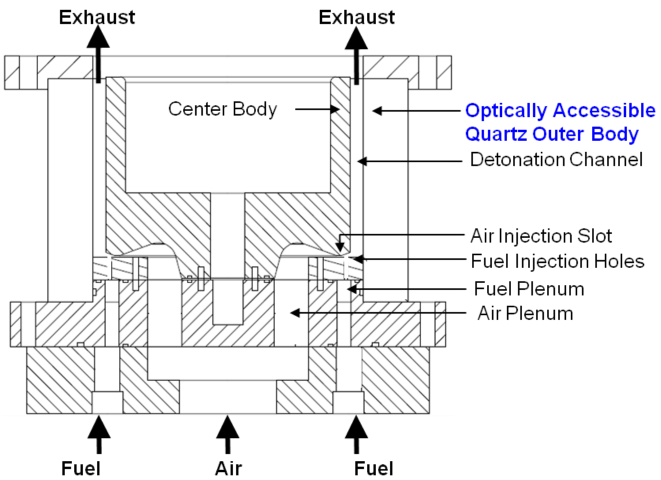

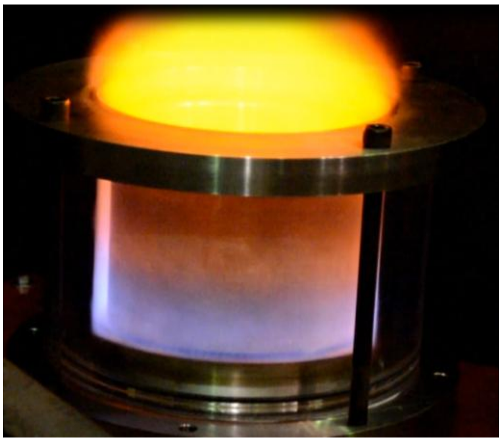

Figure 1. Schematic (left) and photograph (right) of the optically accessible rotating detonation engine.

0.32 kg/s) and high (0.63 and 0.86 kg/s) air mass flow rates, respectively. A gamma correction of 0.5 has been applied to all images reported in this work. The gamma correction applies to regions of the image that have photon count values less than 25% of the maximum camera detection limit.

The OH* chemiluminescence images are post-processed using a spatial transformation to map the azimutal direction onto a plane tangent to the detonation channel. The spatial transformation process results in an “unwrapped” two-dimensional OH* distribution that can be compared with two-dimensional simulations of RDEs. The position of the detonation wave is identified in each instantaneous image using the peak intensity. Phase-averaged images are obtained by averaging approximately 30 instantaneous images that contain a detonation wave within +/- 0.93 mm (3 pixels) of a particular azimuthal position.

3 Results and Discussion

Figure 2 shows instantaneous and phase-averaged images of the OH* chemiluminescence in the optically accessible RDE for four air mass flow rates (0.15, 0.32, 0.61, 0.86 kg/s). The equivalence ratio (1.0), air injection slot (1.78 mm), and fuel injection scheme (0.89 mm – 120) are constant for the images shown in Fig. 4. The field of view of the images spans from the fuel injection surface (y = 0) to the end of detonation channel (y = 10.2 cm) in the vertical direction and includes the region between the outer surfaces of the channel (x = +/- 7.7 cm) in the horizontal direction. The vertical white lines indicate the inner surfaces of the channel (x = +/- 6.9 cm). Regions with low OH* chemiluminescence emissions appear in black, and regions with high OH* chemiluminescence emission appear in white. The instantaneous images are selected randomly from a set of images in which the detonation is near the image centerline. The phase-averaged images are normalized by the maximum phase-averaged intensity for that particular condition to allow for comparison of the size and shape of the detonation wave across the range of operating conditions considered in this work. The direction of propagation for the detonation wave for a particular condition appears to be random with some waves traveling clockwise and others counterclockwise. The images shown in this work have been flipped in the horizontal direction when necessary to allow for a consistent comparison with waves traveling in the same direction. The detonation wave is traveling from right to left using the laboratory frame of reference for all images shown in this work.

The effects of varying the air mass flow rate are evident in Fig. 2. The height of the detonation, as identified by the OH* chemiluminescence emission, initially increases as the air mass flow rate is increased from low (0.15 kg/s) to intermediate (0.32 kg/s) values. Negligible increase in the detonation height is apparent as the air flow rate is further increased to 0.61 kg/s. The detonation transitions from one-wave to two-wave operation as the air flow rate is further increased to 0.86 kg/s resulting in a reduction in the fuel fill height and corresponding detonation height. The instantaneous detonation structure is stochastic regardless of the operating condition with significant variation in the OH* emissions distribution from cycle to cycle.

Figure 3 shows instantaneous and phase-averaged images of the OH* chemiluminescence for three equivalence ratios (0.7, 1.0, and 1.3). The air mass flow rate (0.32 kg/s), air injection slot (0.89 mm), and fuel injection scheme (0.89 mm – 120) are constant for the images in Fig. 3. The detonation wave is present only occasionally for the fuel lean (Φ = 0.7) condition. The detonation wave is apparent consistently for the stoichiometric conditions. The RDE transitions between one and two detonation waves for the fuel rich (Φ = 1.3) condition with the small air slot (0.89 mm) as indicated by the occasional presence of a detonation wave that is twice the height of other waves. The RDE operates primarily with two detonation waves propagating through the channel as demonstrated by the shorter height of the detonation wave in the phase-averaged image. For fuel lean (Φ = 0.7) conditions, the high OH* emissions from the detonation wave are distributed more broadly in space on a phase-average basis. For stoichiometric and fuel rich (Φ = 1.3) conditions, the high OH* emissions from the detonation typically are confined to a more narrow region near the wave front, particularly for the smaller air injection slot (0.89 mm).

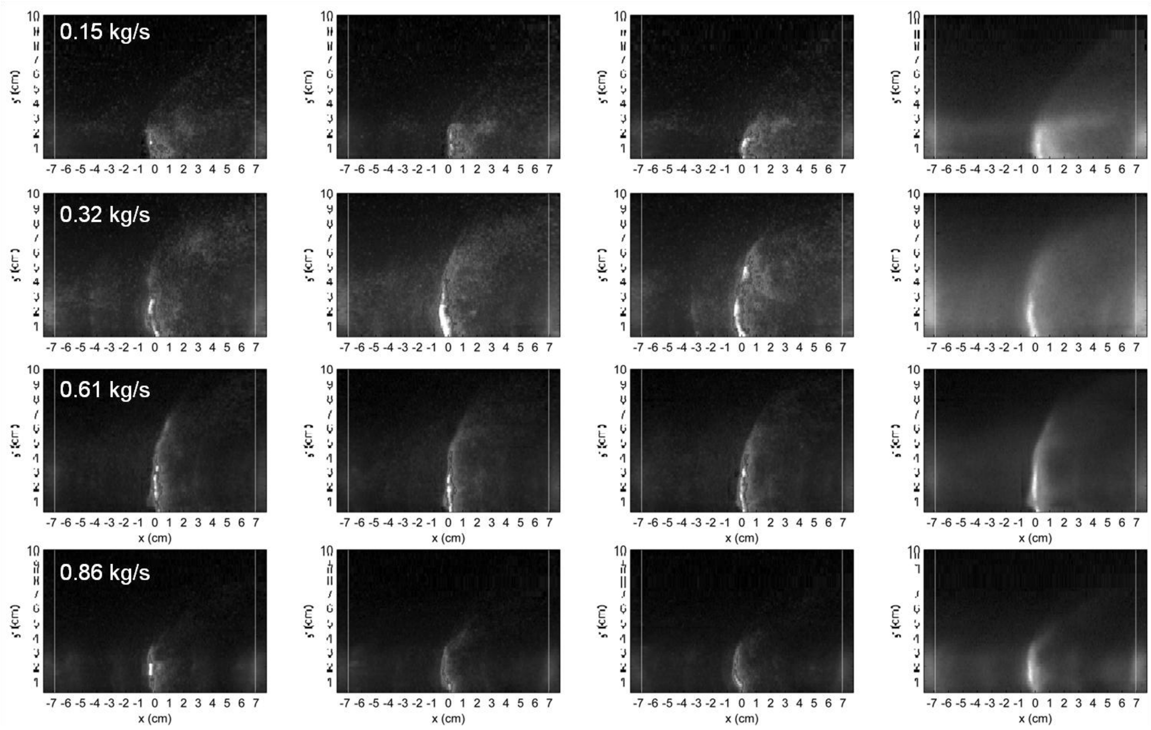

Figure 2. Instantaneous (first, second, and third columns) and phase-averaged (fourth column) images of the OH* chemiluminescence in the RDE for four air mass flow rates (0.15, 0.32, 0.61, 0.86 kg/s). The equivalence ratio (1.0), air injection slot (1.78 mm), and fuel injection scheme (0.89 mm – 120) are constant.

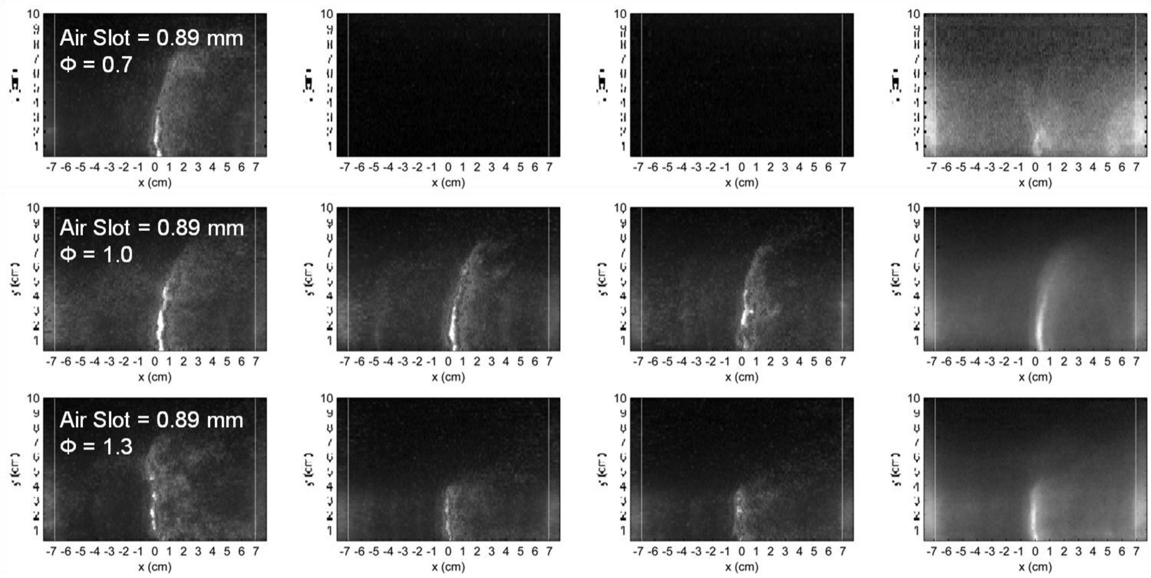

Figure 3. Instantaneous (first, second, and third columns) and phase-averaged (fourth column) images of the OH* chemiluminescence in the RDE operating for three equivalence ratios (0.7, 1.0, and 1.3). The air mass flow rate (0.32 kg/s), air injection slot (0.89 mm), and fuel injection scheme (0.89 mm – 120) are constant.

Figure 4 shows instantaneous and phase-averaged images of the OH* chemiluminescence for three air injection slots (0.89, and 1.78, and 3.56 mm). The air mass flow rate (0.32 kg/s), equivalence ratio (1.0), and fuel injection scheme (0.89 mm – 120) are constant for the images shown in Fig. 4. The wave front appears to be more concave with respect to the fuel fill region in front of the detonation as the air injection slot is increased (from 0.89 to 1.78 mm). The wave front angle becomes more acute with respect to the fuel injection surface in front of the detonation as the air injection slot is further increased (from 1.78 to 3.56 mm).

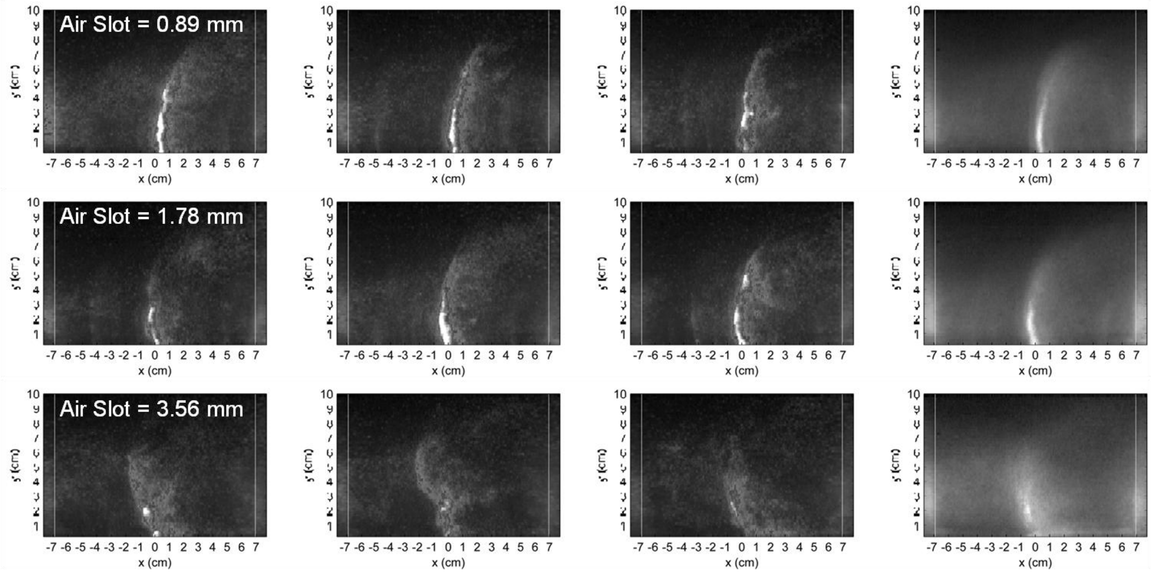

Figure 4. Instantaneous (first, second, and third columns) and phase-averaged (fourth column) images of the OH* chemiluminescence in the RDE for three air injection slots (0.89, and 1.78, and 3.56 mm). The air mass flow rate (0.32 kg/s), equivalence ratio (1.0), and fuel injection scheme (0.89 mm – 120) are constant.

Figure 5 shows instantaneous and phase-averaged images of the OH* chemiluminescence for three fuel injection schemes (0.89 mm – 120, 0.71 mm – 120, and 0.89 mm – 80). The air mass flow rate (0.32 kg/s), equivalence ratio (1.0), and air injection slot (0.89 mm) are constant for the images shown in Fig. 5. Reducing the area of the fuel injection holes (from 0.89 to 0.71 mm) has subtle effects on the height and concavity of the detonation wave front. The mixing between the fuel and oxidizer is impacted by reducing the number of fuel injection holes (from 120 to 80) while maintaining a constant area for each individual hole. The RDE changes from one wave to two-wave operation by reducing the number of fuel injection holes. For conditions in which two-waves are established, the waves typically co-rotate with the detonations propagating in the same azimuthal direction. Counter-rotating waves are observed for stoichiometric conditions with the low air mass flow rate (0.15 kg/s), the small air injection slot (0.89 mm), and the fuel injection scheme with the smaller number of holes (0.89 mm – 80). The observation of two counter-rotating detonation waves demonstrates one occasional effect of non-ideal mixing between the fuel and air in a nonpremixed RDE.

4 Conclusions

Images of the OH* chemiluminescence from detonation waves propagating through the annular channel of an optically accessible nonpremixed rotating detonation engine are acquired, interpreted, and reported for the first time. The primary conclusions from this work are described here.

1) The detonation height increases as the air mass flow rate is increased for relatively low flow rates. Subtle changes are observed in the detonation size and shape for intermediate air flow rates. The RDE transitions from one-wave to two-wave operation as the air flow rate is further increased to relatively high values resulting in a reduction in the fuel fill and corresponding detonation height.
2) The detonation wave is present only occasionally for fuel lean condition near the ignition boundary, present consistently for stoichiometric conditions, and transitions from one-wave and two-waves for fuel rich conditions with a small air slot. For fuel lean conditions, the high OH* emissions from the detonation wave are distributed more broadly in space. For stoichiometric and fuel rich conditions, the high OH* emissions from the detonation typically are confined to a more narrow region near the wave front.

3) The wave front is more concave with respect to the fuel fill region in front of the detonation as the air injection slot is increased from low to intermediate values. The angle between the wave front and fuel injection surface in front of the detonation becomes more acute as the air injection slot is further increased.
4) Reducing the area of the fuel injection holes has subtle effects on the height and concavity of the detonation wave front. Reducing the number of fuel injection holes has significant effects on the detonation structure including transition from one-wave to two-wave operation.
5) For conditions in which two-waves are established in the RDE, the waves typically co-rotate with the detonations propagating in the same azimuthal direction. Counter-rotating waves with the detonations propagating in the opposite azimuthal direction are observed for some operating conditions and geometric configurations. The observation of two counter-rotating detonation waves demonstrates one occasional effect of non-ideal mixing between the fuel and air in a RDE.

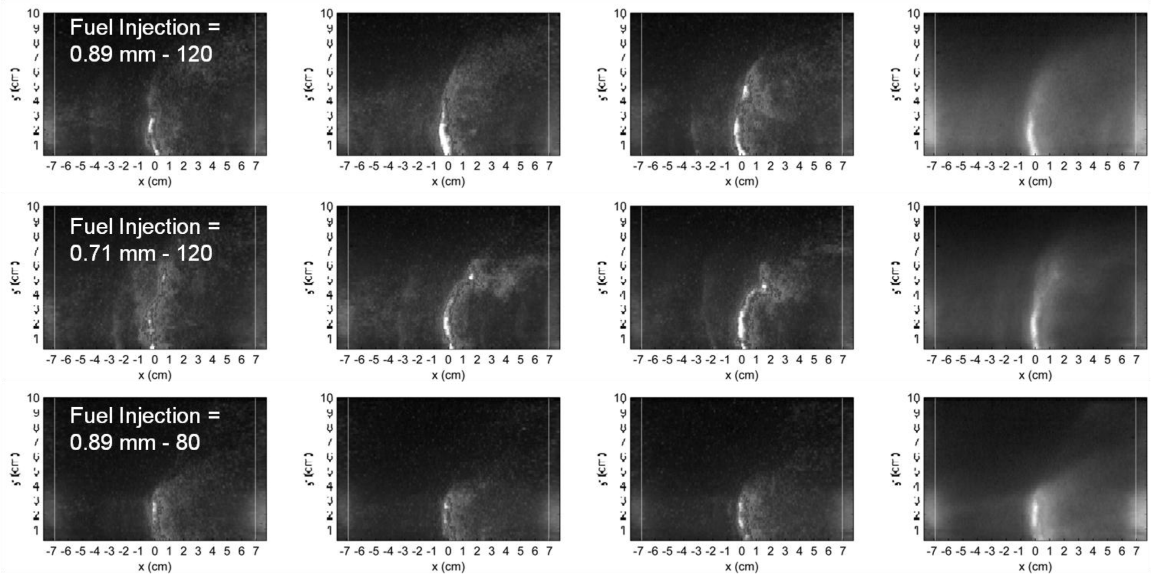

Figure 5. Instantaneous (first, second, and third columns) and phase-averaged (fourth column) images of the OH* chemiluminescence in the RDE for three fuel injection schemes (0.89 mm – 120, 0.71 mm – 120, and 0.89 mm – 80). The air flow rate (0.32 kg/s), equivalence ratio (1.0), and air injection slot (0.89 mm) are constant.

Acknowledgements

This research was performed while Brent Rankin held a National Research Council Research Associateship Award at the Air Force Research Laboratory. The authors would like to thank Justin Goeffena (ISSI), Amy Lynch (AFRL), Curtis Rice (ISSI), and Paul West (ISSI) for their contributions.

References

[1] Wolanski P. (2013). Detonative Propulsion. Proceedings of the Combustion Institute. 34: 125.

[2] Schwer D.A., Kailasanath K. (2013). On Reducing Feedback Pressure in Rotating Detonation Engines. 51st AIAA Aerospace Sciences Meeting. AIAA 2013-1178.

[3] Naples A., Hoke J., Karnesky J., Schauer F. (2013) Flowfield Characterization of a Rotating Detonation Engine. 51st AIAA Aerospace Sciences Meeting. AIAA 2013-0278.

[4] Schwer D.A., Kailasanath K. (2010) Numerical Investigation of Rotating Detonation Engines. 46th AIAA/ASME/SAE/ASEE Joint Propulsion Conference and Exhibit. AIAA 2010-6880.

[5] Paxson D.E. (2014). Numerical Analysis of a Rotating Detonation Engine in the Relative Reference Frame. 52nd AIAA Aerospace Sciences Meeting, AIAA 2014-0284.